SCALING OF e^+e^- STORAGE RING PARAMETERS TO ENERGIES BEYOND LEP

E. Keil, CERN, Geneva, Switzerland

ABSTRACT

The scaling laws of some of the most important machine parameters and phenomena with the design energy are derived for e^+e^- storage rings even larger than LEP. These scaling laws are then used to arrive at likely parameters for such storage rings which are illustrated by a few examples. The difficulties arising are discussed.

1. BASIC RELATIONS

A design procedure for e^+e^- storage rings[1] exists which allows a list of machine parameters to be computed, starting from a relatively small number of assumptions. It is briefly outlined in this section.

The luminosity L obtained when e^+ and e^- beams with N particles each collide head-on is

$$L = \frac{N^2 f}{4\pi k \sigma_x \sigma_y} \tag{1}$$

where f is the revolution frequency, k is the number of bunches in each beam, and σ_x and σ_y are the horizontal and vertical rms beam radii, respectively. In order to obtain a high luminosity it is desirable to keep the beam cross-section $\sigma_x\sigma_y$ small. This leads to the concept of low-β insertions[2] which are included in all storage ring designs. A lower limit on the cross-section arises from the focusing effect of one beam on the other one which is usually expressed in terms of the linear beam-beam tune shift ΔQ. In the horizontal and vertical plane, it is given by

$$\Delta Q_x = \frac{N r_e \beta_x}{2\pi k \gamma (\sigma_x + \sigma_y) \sigma_x} \tag{2}$$

$$\Delta Q_y = \frac{N r_e \beta_y}{2\pi k \gamma (\sigma_x + \sigma_y) \sigma_y} \tag{3}$$

Here r_e is the classical electron radius, β_x and β_y are the horizontal and vertical amplitude functions at the crossing point, and γ is the relativistic factor. Experience with existing e^+e^- storage rings has shown that there is an upper limit[3] on the tune shifts which can be achieved. This limit is called ΔQ.

By using (3) to eliminate one power of N from (1) the following expression is obtained:

$$L \approx \frac{N f \gamma \Delta Q}{2 r_e \beta_y} \tag{4}$$

Here it has been assumed that $\sigma_x \gg \sigma_y$.

If (4) is to be valid and if ΔQ_x and ΔQ_y are both to be equal to ΔQ, the ratio of the beam sizes must be chosen so that

$$\sigma_y/\sigma_x = \beta_y/\beta_x \tag{5}$$

and the horizontal emittance E_x must be chosen as follows:

$$E_x = \sigma_x^2/\beta_x = \frac{r_e^2 \beta_y L}{\pi f k \gamma^2 \Delta Q^2} \tag{6}$$

Suitable lattice parameters to achieve this will be discussed in Section 5. In deriving (6) it has been assumed that the momentum spread does not contribute to the beam size at the crossing points, i.e. that the dispersion vanishes there. There are many good reasons for this choice[4].

An electron which is accelerated transversely with a bending radius ρ emits synchrotron radiation corresponding to an energy loss per unit length given by:

$$\frac{dU}{ds} = -\frac{2}{3}\frac{r_e E_o \gamma^4}{e \rho^2} \tag{7}$$

Here E_o is the electron rest energy, and e its charge. The total loss per turn U_s is therefore, assuming constant ρ:

$$U_s = 2\pi\rho \frac{dU}{ds} = -\frac{4\pi r_e E_o \gamma^4}{3 e \rho} \tag{8}$$

The power P_b which has to be supplied to the two beams is, combining (4) and (8):

$$P_b = \frac{16\pi r_e^2 E_o \beta_y L \gamma^3}{3 \Delta Q \rho} \tag{9}$$

2. SIZE AND COST

It follows from (9) that, for constant L and β_y, the product $P_b\rho$ scales like γ^3. The individual scaling laws for P_b and ρ were obtained by Richter[5] using cost optimization based on unit prices for tunnels equipped with a FODO lattice, tunnels equipped with RF cavities made of copper and operated CW, RF power installations, and electricity cost. Similar procedures were developed by Ritson[6] for pulsed RF systems and Bauer[7] for superconducting ones.

The result of Richter's cost optimization is that the size of a machine, and hence its cost, scales approximately like the square of the energy. The scaling laws for other quantities given below will be based on the assumption that the size scales like E^2 exactly. This result can be made plausible by the following two observations.

In the design of the RF system a balance must be found between the cost of the cavities which is proportional to their length L_c, and the cost of the RF power which is

proportional to $1/L_c$ when the RF power delivered to the beam is ignored. It is intuitively obvious that the balance is obtained at a given voltage gradient, independent of the machine energy. The optimum gradient is quite low, about 1 MV/m, far below the breakdown limit of copper cavities. The cavity length is proportional to the synchrotron radiation loss, $L_c \sim U_s$ if the variation of the stable phase angle with energy and the higher-mode voltage U_{hm} are neglected.

In the design of the whole machine an optimum must be found between the total cost of the whole RF system and the cost of the bending arcs. Here it is intuitively obvious that this optimum is reached when the fraction of the machine circumference occupied by the RF system is independent of the energy, i.e. when the machines are similar, and ρ and L_c scale in the same manner, as long as the unit prices are independent of the energy. Since the synchrotron radiation loss $U_s \sim E^4/\rho$, the product ρL_c scales like E^4, and ρ and L_c scale like E^2.

3. RF SYSTEM

From the scaling laws it is known that the length of the RF system scales like E^2. It follows from (9) that the synchrotron radiation power scales like $EL\beta_y/\Delta Q$. Further parameters of the RF system are discussed in this section.

3.1 RF power

The total RF power which has to be supplied by the power sources is made up of several contributions, the dissipated power in the cavities P_d, the synchrotron radiation power P_b, the higher-mode power P_{hm}, and the reflected power due to the transient beam loading. In a CW RF system the largest fraction is the dissipated power P_d which scales like E^2. The synchrotron radiation power P_b scales like $EL\beta_y/\Delta Q$.

Since P_b scales with a lower power of E than P_d, the fraction of the total RF power transferred into the beam decreases with energy if the other parameters remain the same. This is a good reason to look for alternatives to copper cavities driven by CW power sources. Two alternatives have been proposed. Pulsing the power sources[8] might become attractive when the time between bunches becomes long compared to the RF filling time. Superconducting RF cavities would reduce the dissipation by a large factor.

The higher-mode losses are due to the excitation of electro-magnetic fields in the cavities by the passage of the short intense bunches. They have two effects on the RF power requirements. The power P_{hm} corresponding to them has to be supplied to the beams. At a given frequency and bunch length it scales like $(L\beta_y E/\Delta Q)^2/k$, but is usually negligible. The second effect is the additional dissipated power because the cavity voltage has to be increased to compensate the higher-mode voltage U_{hm}. At a given frequency and bunch length $U_{hm} \sim E^3 L\beta_y/(k\Delta Q)$. As long as $U_{hm} \ll U_s$, the dominant term in the additional dissipation scales like $E^3 L\beta_y/(k\Delta Q)$, i.e. more steeply than P_d.

With a constant RF voltage gradient the stored energy per unit length in the cavities depends only on the RF frequency. On the other hand, the energy which has to be supplied to the beam, per unit length, in a single passage through the cavities, is proportional to N/k. Hence the ratio between extracted and stored energy scales like $EL\beta_y/\Delta Qk$.

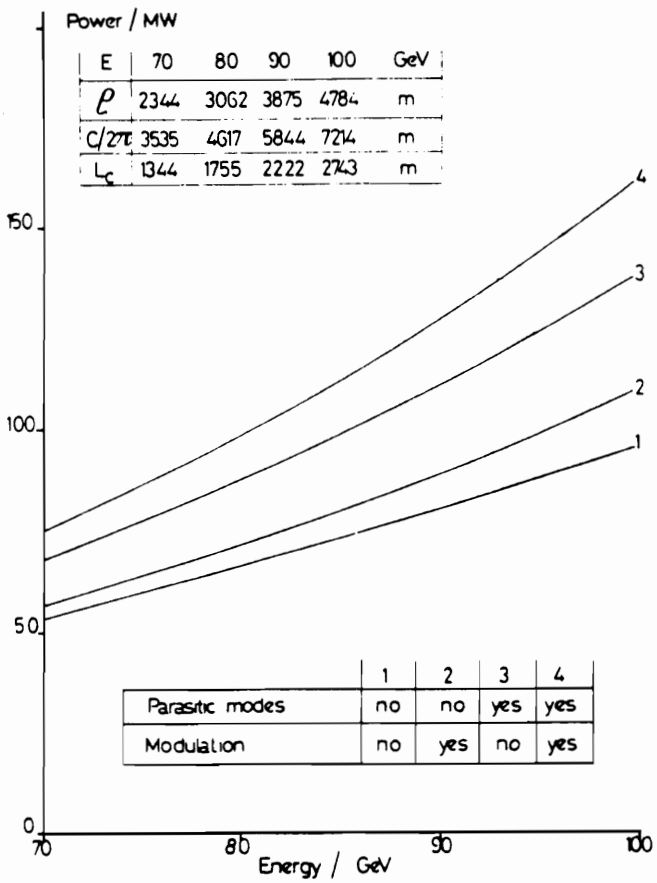

Fig. 1. RF generator power vs. design energy

The consequences of all these observations cannot be expressed as a simple power law in a few variables. However, the standard transient beam-loading calculation[9] automatically takes care of them; the result for a sample of machines is shown in Fig. 1. It is scaled from LEP-70, and assumes constant L, β_y, k and ΔQ and no storage cavities. The lowest curve just gives the sum $P_b + P_d$ when the higher-mode losses vanish, the second curve includes the transient beam loading, the third curve includes the higher-mode losses but not the transient beam loading; the top curve includes everything. It is clear that the most simple-minded approach, the bottom curve, can lead to considerable underestimates in the total RF power.

3.2 Synchrotron tune Q_S

So far, it has been tacitly assumed that the frequency was about constant in the scaling operation. In existing machines it was largely chosen bearing in mind the availability of high-power RF sources and the cost of RF cavities. In addition to beam loading, there are several other phenomena which favour a lower frequency. One of them is synchro-betatron resonances which can occur when the betatron tune Q and the synchrotron tune Q_S of a machine are related by

$$Q \pm nQ_S = p \qquad (10)$$

where n and p are positive integers. In machines like SPEAR[10] and PETRA[11] crossing them is associated with beam loss. In order to avoid them the working point Q has to be chosen carefully and controlled very well. Synchro-betatron resonances can be driven by dispersion in the RF cavities[12]. In this case their strength increases with Q_S. For $Q_S \ll 1$, it scales like $Q_S^{3/2}$. In an ideal machine, the dispersion can be made zero in the RF system. However, errors in the positioning and strengths of the magnetic elements

will always cause small but finite values of the horizontal and vertical dispersion. Synchro-betatron resonances can also be driven by exciting transverse deflecting fields in the RF cavities and other similar objects when the bunches pass them off-axis[13]. It is easy to relate Q_s to the performance parameters of the machine:

$$Q_s \geq \left(\frac{2r_e}{c}\right)\left(\frac{4\pi^3\, r_e\, c}{27\, C_q^{\,2}}\right)^{1/6} (-f_{RF} R \cot \phi_s)^{1/2} \left(\frac{\gamma}{\rho}\right)^{1/6} \left(\frac{\beta_y L}{k\, \Delta Q^2}\right)^{1/3} \qquad (11)$$

Here, c is the velocity of light, $C_q = 3.84\times10^{-13}$m, and ϕ_s is the stable phase angle. The equals sign applies when higher-mode losses are neglected. In deriving (11) it has been assumed that the emittance is adjusted by an appropriate choice of the tune, according to (16), and not by wiggler magnets[14] and/or a variation of the damping partition numbers[15]. It follows that for constant Q_s, f_{RF} has to scale as follows:

$$f_{RF} \sim E^{-5/3} (k\, \Delta Q^2/\beta_y L)^{2/3} \qquad (12)$$

In order to keep Q_s constant the frequency has to scale like $E^{-5/3}$ at constant k; or k has to be increased like $E^{5/2}$ at constant f_{RF}. In the latter case the bunch spacing decreases because k increases faster than the machine size.

Pulsed travelling-wave RF systems look most attractive when the frequency and the bunch spacing are high[8]. This requirement conflicts with the above condition for constant Q_s.

4. INTERACTION REGION DESIGN

4.1 Limits on β_y

In order to obtain the desired luminosity with the minimum circulating current, the design of e^+e^- storage rings includes low-β insertions which make the beam size at the interaction point particularly small. This has several consequences which will be discussed in this section.

The consequences of optical limitations on the design of the interaction regions[16] can be qualitatively discussed in the following way. The rms beam size at the crossing point is known. In thin-lens approximation it can be extrapolated to the centre of the nearest quadrupole which is at a distance ℓ_x from the crossing point. Constraints on ℓ_x due to the size of experiments are ignored for the time being. The aperture of this quadrupole must be a factor $F_a \approx 10$ larger than the rms beam size in it. The quadrupole field at the edge of the aperture B_Q is determined by its construction technique, $B_Q \approx 1$ T for a copper-steel quadrupole and higher for a superconducting one. In order to obtain the focal length imposed by the optics, which is roughly $\frac{1}{2}\ell_x$, the physical quadrupole must have a length ℓ_Q. Optics prohibits too small ratios $G_\ell = \ell_x/\ell_Q$, we use $G_\ell = 1.5$. Finally, the chromatic effects of the quadrupole must be considered. Since

they must be corrected for a momentum bite of about ± 1%, the ratio $G_c = \ell_x/\beta_y$ cannot be larger than 50 to 100. Applying all these considerations yields a formula for β_y :

$$\beta_y = \frac{G_\ell F_a}{G_c} \frac{e Z_o}{2\pi B_Q \Delta Q} \left(\frac{L \beta_y}{\pi k f \beta_x} \right)^{\frac{1}{2}} \qquad (13)$$

Here $Z_0 = 120\pi\Omega$ is the impedance of free space. On the right-hand side only the ratio β_y/β_x appears. If the aperture calculation had been done for full coupling, this factor would have dropped out. Applying equ. (13) to the high-luminosity LEP insertion gives good agreement. It implies that $\beta_y \sim E$ if all other terms are kept constant. Constant β_y could be achieved by having $k \sim E^2$, a less steep variation than that required by the synchrotron tune Q_s (Section 3.2).

4.2 Phenomena related to synchrotron radiation

Two other phenomena entering into the design of the interaction regions are related to synchrotron radiation. Any electron which is deflected emits synchrotron radiation. This also holds for particles which pass a quadrupole field off-axis. This happens in two places in an interaction region, in the field of the opposite beam, and in the quadrupole magnets. Since the curvature in a quadrupole is proportional to the distance from the axis, these phenomena depend on the particle amplitude. Here they are calculated for one standard deviation.

4.2.1 Beam strahlung

The first phenomenon[17] was dubbed "beam strahlung". In this case the bending radius is relatively small and the interaction length is comparable to the bunch length σ_z. This implies that the critical photon energy is high and the number of photons emitted by one particle in a collision is low. Therefore the dominant effect of beam strahlung is a contribution to the energy spread of the beam. If the condition is imposed that this contribution be no larger than the energy spread in the absence of beam strahlung, the following relation must be satisfied:

$$L^{3/2} E^4 n_x/\sigma_z^2 k^{3/2} \leq 10^{66} \qquad (14)$$

Here n_x is the number of crossing points. Distances are measured in metres, the energy in GeV, and $10^{32} cm^{-2} s^{-1} = 10^{36} m^{-2} s^{-1}$. Equ. (14) is independent of the beam-beam limit ΔQ, but assumes as in LEP that the ratio of the beam sizes at the crossing points is $\sigma_y/\sigma_x = 0.06$. For parameters similar to those of LEP, $L = 10^{32} cm^{-2} s^{-1}$, $n_x = 8$, $k = 4$, $\sigma_z = 0.063$ m we find $E \approx 250$ GeV. This limit is probably pessimistic because of the approximations used in calculating the curvature. If beam strahlung is not to be a problem at higher energies, the bunch length σ_z and/or the bunch number k must be increased.

4.2.2 Quadrupole radiation

The quadrupole radiation as it shall be called here is mainly generated in the insertion quadrupoles. Its characteristics differ from those of the beam strahlung. The bending radius and hence the critical photon energy are more comparable to those in the dipoles. In addition the length of the quadrupole is much higher than the bunch length and hence the number of photons emitted by one particle when passing the quadrupole is higher. Therefore the dominant effect of quadrupole radiation is its contribution to the energy loss, while its contribution to the energy spread is negligible.

By arguing about the quadrupole aperture and strength in the same way as in Section 4.1 one can obtain an expression for the ratio of the synchrotron radiation losses in an interaction region quadrupole U_Q to those in the bending arcs U_S:

$$U_Q/U_S = \frac{r_e\, c\, e}{\pi\, E_o} \frac{B_Q\, \rho}{F_a\, \gamma^2\, \Delta Q} \left(\frac{L}{2\pi\, f\, k}\right)^{\frac{1}{2}} \tag{15}$$

The stable phase angle now becomes a function of the betatron amplitude[18]. Other consequences of quadrupole radiation are being studied[19]. With all parameters except f fixed and with $f \sim E^{-2}$, $U_Q/U_S \sim E$. If $k \sim E^2$, the ratio U_Q/U_S becomes a constant.

Both beam strahlung and quadrupole radiation are potential sources of background for experiments installed in the interaction regions.

5. MAGNET LATTICE

The bending radius ρ and the overall radius R of the arcs are known to scale like E^2. The emittance E_x is given by (6). In this section, the standard method[1] of obtaining this emittance is discussed, and the aperture of the magnet lattice is estimated.

5.1 Tune

The emittance E_x in an e^+e^- storage ring is the result of a balance between the beam growth due to quantum excitation and synchrotron radiation damping. It can be controlled by choosing the dispersion in the magnet lattice whose average value is R/Q^2. Here Q is the contribution of the arcs to the tune of the machine. The condition (6) yields an expression for the value of Q[1]:

$$Q^3 = \frac{C_q\, e}{2J_x\, r_e^2} \frac{\gamma^4\, k\, \Delta Q^2}{\rho\, \beta_y\, L} \tag{16}$$

Here $J_x \approx 1$ is the damping partition number for horizontal betatron oscillations. Eq. (16) applies for not too large phase advances μ per period. An accurate derivation valid for all values of μ is given in ref. 20.

Assuming that L and ΔQ do not depend on the energy it follows that Q scales like $(E^2 k/\beta_y)^{1/3}$.

5.2 Aperture

The length of a lattice period L_p is given by

$$L_p = R\mu/Q \tag{17}$$

It determines the maximum value of the amplitude function ß

$$\hat{\beta} = \frac{L_p}{2 \tan \frac{\mu}{2} \left(1 - \sin \frac{\mu}{2}\right)} \tag{18}$$

Combining (18) with the emittance given by (6) allows a calculation of the rms beam size, and of the half size of the vertical aperture A_y which is usually chosen a factor $F_a \approx 10$ larger than the beam size:

$$A_y = F_a(\tfrac{1}{2} E_x \hat{\beta})^{\frac{1}{2}} = F_a \left[\frac{2^{1/3}}{4\pi} \frac{r_e^{8/3}}{(C_q c)^{1/3}} \frac{R}{f} \left(\frac{\beta_y L}{k}\right)^{4/3} \frac{(\rho J_x)^{1/3}}{\gamma^{10/3} \Delta Q^{8/3}} \right]^{1/2} \tag{19}$$

Here the fact has been used that the vertical emittance is at most $E_x/2$, in the fully coupled case. It has also been assumed that the phase advances μ_x and μ_y are about equal. Under these assumptions the horizontal half aperture is about $3^{1/2} A_y$. If L and ΔQ are again assumed to be constant, it follows that A_y scales like $(E\beta_y/k)^{2/3}$.

The scaling laws (16) for the tune, (17) for the lattice period L_p, and (19) for the aperture imply a certain scaling law for the lattice quadrupole field at the edge of the aperture. The scaling laws for the machine size imply that the fraction of a lattice cell occupied by the quadrupoles is constant. It can be shown explicitly that these two sets of conditions can be met with a quadrupole field at the edge of the aperture, B_Q which is inversely proportional to the energy.

5.3 Bunch length

At this point, all the data are available to calculate the nominal bunch length σ_{zo} for vanishing current. Bunch lengthening will be considered in Section 6.1. The bunch length is given by

$$\sigma_{zo} = \frac{\alpha C \sigma_{eo}}{2\pi Q_s} \tag{20}$$

Here α is the momentum compaction, C is the machine circumference, and σ_{eo} is the natural energy spread due to quantum excitation and radiation damping:

$$\sigma_{eo} = \gamma \left(\frac{C_q}{\rho J_s} \right)^{\frac{1}{2}} \tag{21}$$

Here $J_s \approx 2$ is the damping partition number for synchrotron oscillations. The momentum compaction is:

$$\alpha = \frac{2\pi R}{CQ^2} \tag{22}$$

Combining (20), (21) and (22), the bunch length becomes

$$\sigma_{zo} = \frac{\gamma R}{Q^2 Q_s} \left(\frac{C_q}{\rho J_s} \right)^{\frac{1}{2}} \tag{23}$$

Substituting (11) for Q_s and (16) for Q and arranging terms, the following result is obtained

$$\sigma_{zo} = \left(\frac{C_q c r_e}{2} \right)^{1/6} \left(\frac{J_x^2 \beta_y L \rho}{k \Delta Q^2} \right)^{1/3} \left(\frac{3R}{2\pi J_s f_{RF} \cot \phi_s} \right)^{1/2} \gamma^{-11/6} \tag{24}$$

Assuming that L and ΔQ are kept constant, and neglecting any variation of the stable phase angle ϕ_s, it follows that σ_{zo} scales like $(\beta_y/k)^{1/3} f_{RF}^{-1/2} E^{-1/6}$.

6. COLLECTIVE PHENOMENA

6.1 Bunch lengthening

Bunch lengthening and widening is observed in all operating e^+e^- storage rings. As suggested by the names, the length and the energy spread of the bunches for finite current I are larger than for vanishing current. The reason for this is believed to be a turbulent instability[21], driven by the impedance which the vacuum chamber and the RF system present to the beam. The same impedance also causes the higher-mode losses discussed in Section 3.1.

The energy spread σ_e due to the turbulent instability is given by

$$\sigma_e^3 = \frac{Q_s}{\alpha^3} \frac{(2\pi)^{\frac{1}{2}} I}{k h V_{RF}} \left| \frac{Z/n}{\cos \phi_s} \right| \tag{25}$$

Here h is the harmonic number, V_{RF} is the peak voltage of the RF system and Z/n is the impedance divided by the mode number n, taken at the most efficient frequency exciting turbulent bunch lengthening, i.e. about c/σ_z. The mode number is the ratio between that frequency and the revolution frequency.

In a modern machine with a rather smooth vacuum chamber, Z/n is dominated by the contribution of the RF system and typically amounts to a few Ω. Bunch lengthening occurs when the energy spread given by (25) exceeds the natural energy spread σ_{eo} given by (20).

If one observes that the quantities occurring in (25) are related to performance parameters such as L, β_y and ΔQ, and if one assumes that the machine parameters are adjusted accordingly, one finds for the bunch lengthening $B = \sigma_e/\sigma_{eo}$:

$$B^3 = \frac{e^2 c}{E_o} \frac{\Delta Q \, |Z/n|}{J_x} \left(- \frac{\gamma h \cot \phi_s}{3\pi r_e C_q} \right)^{1/2} \left(\frac{J_s C}{2\pi R} \right)^{3/2} \qquad (26)$$

The surprising feature of (26) is the absence of parameters such as L, β_y, or k. The significant parameters for B are ΔQ, γ and h. Since $h \sim E^2 f_{RF}$ we conclude that B scales like $E f_{RF}^{1/3}$. In order to keep B constant the RF frequency f_{RF} has to be decreased like E^{-3}. For a given energy, a machine with a superconducting RF system has about half the radius of a machine with a conventional CW RF system[7]. Hence, for equal bunch lengthening B and energy E, the radio frequency f_{RF} can be a factor of two higher in a superconducting machine. For equal B and f_{RF}, the energy E in a superconducting machine can be higher by a factor $2^{1/3} \approx 1.26$. By combining the scaling laws (24) for the natural bunch length σ_{zo} and (26) for B one finds that σ_z scales like $(\beta_y E/k f_{RF})^{1/3}$.

6.2 Coherent tune shift

The most dangerous transverse phenomenon in LEP[4] is the real frequency shift $\delta Q_{m=0}$ associated with the head-tail instability in a single beam. Since the incoherent tune shift of a single beam is small, a difference arises between the two tunes which is proportional to the circulating current I. It must not exceed the value one half.

An estimate for $\delta Q_{m=0}$ is given by

$$\delta Q_{m=0} = \frac{I R^2 Z_T}{8 k Q E \sigma_z} \qquad (27)$$

Here Z_T is the effective transverse impedance which can be related to the longitudinal impedance Z by[22]

$$Z_T(\omega) \approx \frac{2R}{A_y^2} \frac{Z(\omega)}{n} \sim R A_y^{-3} \qquad (28)$$

where n is the mode number. Since Z/n is about proportional to A_y^{-1}, the transverse impedance Z_T scales like $R\ A_y^{-3}$. Substituting the scaling laws (4) for I, (16) for Q, (19) for A_y, (24) for σ_{eo}, and (26) for B yields the following scaling law for $\delta Q_{m=0}$:

$$\delta\ Q_{m=0} \sim (Ek/\beta_y)\ (L/\Delta Q)^{4/3}\ f_{RF}^{1/3} \tag{29}$$

At first sight, this scaling law looks quite strange, since $\delta Q_{m=0}$ is inversely proportional to β_y and proportional to k. This behaviour can be understood by observing that the scaling law is dominated by the dependence of the aperture A_y (19) on these parameters.

7. CONCLUSIONS

In order to find our way through the constraints on the machine design imposed by the various phenomena discussed above, we want to express them in terms of the smallest possible set of parameters. For simplicity we assume that L and ΔQ are kept constant. If we eliminate the bunch length σ_z from (14) by using (24) and (26), i.e. by estimating beam strahlung for lengthened bunches, we can express all scaling laws in terms of only four parameters: E, f_{RF}, k, β_y^*, as shown in Table 1.

Table 1.

Summary of scaling laws

No.	Constant	Requires
1	Bunch lengthening	$f_{RF} \sim E^{-3}$
2	Quadrupole radiation	$k \sim E^2$
3	β_y^*	$k \sim E^2$
4	Q_s	$f_{RF}(\beta_y/k)^{2/3} \sim E^{-5/3}$
5	Beam strahlung	$k^{5/4}(\beta_y/f_{RF}) \sim E^5$
6	$\delta Q_{m=0}$	$(k/\beta_y)f_{RF}^{1/3} \sim E^{-1}$

The first constraint, due to bunch lengthening, imposes a condition on the radio frequency f_{RF}. As the frequency decreases, the cost of the RF cavities and of the power sources increases rapidly. If we assume that a practical lower limit is f_{RF} = 50 MHz and if we are willing to tolerate the same bunch lengthening as in LEP, we find a maximum design energy of E = 165 GeV for a copper RF system, or E = 210 GeV for a superconducting RF system at the same frequency. For f_{RF} = 100 MHz, the corresponding energies are 130 GeV and 165 GeV, respectively. It follows from (26) that the bunch lengthening factor B is proportional to the sixth root of $E^3 f_{RF}$. Hence, the limiting energies can be increased by assuming a slight increase in B.

The second and third constraints relate the number of bunches to the energy. They imply that the bunch spacing must be constant. It follows that the e^+ and e^- beams must be separated by electrostatic plates if they circulate in a single magnet lattice, or that they must circulate in two different magnet lattices. In either case, they must be made to collide with tight tolerances at the crossing points. This conclusion was already reached in ref. 17) for different reasons. Both schemes deviate drastically from present schemes with $k = n_x/2$ in which the collisions between e^+ and e^- bunches are ensured by the CPT theorem.

The fourth and fifth constraints are automatically satisfied if the above conditions on f_{RF} and k are fulfilled.

When the scaling laws $f_{RF} \sim E^{-3}$ and $k \sim E^2$ are applied to the last constraint it follows that $\delta Q_{m=0} \sim E^2$ which is not acceptable. However this difficulty can be circumvented, by changing the scaling law for the vertical aperture A_y. It was already noted at the end of Section 5.2 that a constant "filling factor" ρ/R can be achieved with a quadrupole field B_Q which is inversely proportional to the energy. The obvious alternative is to keep B_Q constant and to add one power of E to the scaling law for the aperture (19). At constant L, β_y and ΔQ, and with $k \sim E^2$, the aperture scales like $E^{1/3}$ and hence doubling the energy only requires a rather modest increase in the aperture. This change in the aperture adds a factor E^{-3} to the right-hand side of (29), and ensures that $\delta Q_{m=0}$ decreases with energy.

The scaling laws derived above were used to study the parameters of a machine having four times the size of LEP[4] and having twice the energy of Stage II in LEP, 260 GeV. A short parameter list is given in Table 2 which should be largely self-explanatory. The beam strahlung parameter is the left-hand-side of (14). The parameters were computed by the DESIGN program which includes most of the formulae in this paper, and exact beam loading and quantum lifetime calculations. It should be noted that the synchrotron radiation loss per turn amounts to more than 10% of the particle energy.

It turned out that the assumption of constant RF phase angle ϕ_s was too rough. With increasing energy, ϕ_s approaches $\pi/2$ and cot ϕ_s becomes smaller. Hence the computed values of Q_s and B are smaller, and those of σ_{zo} and σ_z are larger than the values obtained from the scaling laws at constant ϕ_s.

Table 2.

Parameters of 260 GeV e^+e^- storage ring

Energy	E	260	GeV
Number of crossings	n_x	8	
Number of bunches	k	16	
Circumference	C	126	km
Average radius of lattice cells	R	16	km
Bending radius	ρ	14	km
Betatron tune (arcs only)	Q	257	
Phase advance/cell	μ	60°	
Period length	L_p	65.2	m
Dipole field	H	0.062 T	
Max. and min. amplitude functions	β	112.9 37.6	m
Max. and min. dispersion	D	0.33 0.20	m
Max. hor. and vert. rms beam radius in cell		1.06 0.22	mm
Natural rms energy spread	σ_{eo}	1.88×10^{-3}	
Natural bunch length	σ_{zo}	19.9	mm
Bunch lengthening factor	B	3.4	
Actual bunch length	σ_z	67.4	mm
Hor. and vert. amplitude functions at crossings	$\beta_{x,y}$	1.6 0.1	m
Luminosity	L	10^{32} $cm^{-2}s^{-1}$	
Free space around crossings	ℓ_x	5	m
Beam-beam tune shift	ΔQ	0.06	
Hor. and vert. rms beam radius at crossing	σ_x, σ_y	100 6.3	μm
Beam strahlung parameter		1.26×10^{65}	
Circulating current/beam	I	2.78	mA
Synchrotron radiation loss per turn	U_s	28.9	GeV
Synchrotron radiation power (two beams)	P_b	161	MW
Length of RF system	L_c	7.5	km
RF frequency	f_{RF}	50	MHz
Peak RF voltage	V_{RF}	29.1	GV
Stable phase angle	ϕ_s	96.6°	
Synchrotron tune	Q_s	0.023	

The design of high-luminosity e^+e^- storage rings does not become easier with increasing energy, even though most of the technical problems encountered in the design of LEP-100[23] were not considered here. The best solution found, a machine with many bunches in each beam and an RF system with a much lower frequency than presently favoured values, is not attractive. In addition, the cost of storage rings is likely to increase roughly in proportion to the square of the energy.

These features of an e^+e^- storage ring should be compared with those of colliding linacs[24]. Firstly, the cost of colliding linacs might be expected to be proportional to the energy. Secondly, they do not seem to be so prone to slow collective phenomena as storage rings. On the other hand, the art of building and operating storage rings has been developed over the last 15 years during which the difficulties which appeared have only gradually and partially been solved. Serious work on colliding linacs was only started about two years ago, no actual machine has so far been built, and much remains to be learned in this field. Storage rings designers are only too acutely aware of the unexpected problems that can arise when a new concept is put into practice.

* * *

REFERENCES

1) J.R. Rees and B. Richter, SPEAR-167 (1973).

2) K. Robinson and G.A. Voss, CEA-TM-149 (1965).

3) E. Keil, CERN Int. rep. ISR-TH/79-32 (1979).

4) The LEP Study Group, Int. rep. CERN-ISR-LEP/79-33 (1979).

5) B. Richter, Nucl. Instrum. Methods, 136, 47 (1976).

6) D. Ritson, PEP Note 280 (1979).

7) W. Bauer, in CERN 79-01, 351 (1979).

8) P.B. Wilson, IEEE Trans. Nucl. Sci. NS-26, 3255 (1979).

9) P.B. Wilson, Proc. 9th Internat. Conf. on High Energy Accelerators, Stanford, 1974 (CONF 740522, USAEC, Washington, 1974) 57.

10) SPEAR Group, IEEE Trans. Nucl. Sci. NS-24, 1863 (1977).

11) G.A. Voss, private communication.

12) A. Piwinski and A. Wrulich, DESY 76/07 (1976).

13) R.M. Sundelin, IEEE Trans. Nucl Sci. NS-26, 3604 (1979).

14) I.M. Paterson, J. Rees and H. Wiedemann, SPEAR-186, PEP-125 (1975).

15) G.A. Voss, IEEE Trans. Nucl. Sci. NS-26, 2970 (1979).

16) E.D. Courant and E. Keil, Proc. Workshop on Possibilities and Limitations of Accelerators and Detectors, Fermilab October 1978, 135 (1979).

17) J.-E. Augustin et al., ibid, 87.

18) A.W. Chao and A.A. Garren, PEP Technical Memo 141 (1978).

19) M. Bassetti, private communication.

20) R. Helm and H. Wiedemann, PEP-303 (1979).

21) D. Boussard, CERN Int. rep. Lab. II/RF/Int./75.2 (1975).

22) W. Schnell, CERN Int.rep. ISR-RF/70-7 (1970).

23) J.R.J. Bennett et al., CERN Report 77-14 (1977).

24) U. Amaldi, Int. rep. CERN-EP/79-136 (1979) and Proc. of the 1979 Int. Symposium on Lepton and Photon Interactions at High Energies, 1979 (eds. T.B.W. Kirk and H.D.I. Abarbanel) (FNAL, Batavia, 1979), p. 314-326.